EXPERIMENTAL AND NUMERICAL STUDY OF TWO FIRST HIGHLY-LOADED STAGES OF COMPRESSORS AS A PART OF HPC AND SEPARATE TEST UNIT

V.I. Mileshin, P.G. Kozhemyako, I.K. Orekhov, V.A. Fateev*
***Central Institute of Aviation Motors (CIAM)**
2, Aviamotornaya st., 111116, Moscow, RUSSIA
E-mail: mileshin@ciam.ru

Keywords: *experimental and numerical investigations, advanced HPC*

Abstract

In current paper the results of experimental and numerical investigation of two versions of two first highly-loaded high efficiency stages of advanced HPC are represented.

First version is dealing with the results of experimental and numerical investigation of separate two stages compressor with the pressure ratio π^*_c=3.7.

Second version is dealing with the results of experimental and numerical investigation of 8-stages HPC including two first compressor stages with the pressure ratio $\pi^*_c \approx 3.5$ and mass flow rate on 7% less in comparison with the first variant.

Two first stages of both compressors have approximately the same ratio π^*_c/G_{cor}, although the design features differ significantly.

During design and computation of compressor performances modern 3D mathematical models based on through flow calculations of 3D viscous flow on base of Navier-Stokes equations were applied [1-5]. Also 3D-inverse solver [2, 4, 5] was used for optimization of blade row profiling taking into account the specified optimal load distribution.

After optimization of blade row profiling on base of 3D-inverse solver the analysis of flutter, static and dynamic behavior was carried out. Usually it is necessary to have 2-3 iterations between gas dynamic and mechanical designs to provide required gas dynamic and mechanical performances of the stages.

Besides, the paper represents the experimental results of local and integral characteristics investigations for two first compressor stages as a part of 8-stage high pressure compressor and separate test unit.

The numerical results, defined on base of 3D viscous flow, corresponds quite satisfactory with the experimental results.

Nomenclature

HPC – high pressure compressor
IGV – inlet guided vane
Z – number of blades, or HPC stages
$\bar{h}=h/b_{middle}$ - blade extension;
h - blade height; b - blade chord;
ρ - density; a – sound speed;
M – Mach number; R1, R2 – Rotor1, Rotor2;
S1, S2, S3 – Stator1, Stator2, Stator3;
T – temperature; P – static pressure ($P/\rho_0 \cdot a_0^2$);
DL – Liblein diffusion factor;
MP1, MP2, MP3 – “mixing plane” before R1, S1 and R2 correspondingly
U_{tip} – R1 tip rotational speed;
$\bar{d}$ – relative diameter; π^* – total pressure ratio;
η^*_{ad} – adiabatic efficiency;
$\bar{n}$ [%] – relative rotor spool speed;
$\bar{d}_1$ – relative hub diameter.

Introduction

One of the crucial problems arising in designing of few-stage high-pressure compressors (HPC) is the well-grounded choice of principles for distribution of parameters among the stages and, respectively, the choice the stage configuration.

As a result of the comparative analysis of calculated performances for several HPC versions, it is found that the most promising layout is the HPC with extremely high aerodynamic loading of the first two stages. This HPC layout ensures a decrease of aerodynamic loading in other stages and makes easier the problem how to provide acceptable levels of efficiency and surge margin.

Because of minimal number of stages in HPC, the high-loaded stages should provide high theoretical head coefficients ($\bar{H}_T$>0.4 on average). It means that their specific feature is high aerodynamic loading with a proper level of diffusion factors of stators and rotors (DL> 0.5). The mean value of another criterion - $\bar{H}_T/\bar{C}1a$ complex parameter - should be very close to 1.

1 Numerical and experimental analysis of high-loaded compressor HPC2 simulating first two stages a high-loaded HPC

The success in developments of advanced compressors depends, to a great extent, on the degree of sophistication of its high-loaded first and second stages. Therefore, primary emphasis is placed on studies of these stages. This work presents an example of mathematical and experimental investigations of a highly-loaded two stages compressor HPC2 which will be used as the basis for development of first two stages for a typical HPC.

Data of three-dimensional viscous flow calculations by"3D-IMP-MULTI" software package for integration of Navier-Stokes equations (the software was developed by CIAM's Compressor Department) are used for the mathematical analysis [3]. Wilcox k-ω differential model is used for turbulent viscosity calculations [3-4].

Two stages compressor HPC2 shall provide the following design parameters at $\bar{n}_{cor}$=100%, $u_{1R\ tip}$ = 441 m/s, $\bar{d}_1$=0.652:

Total pressure ratio of the 1 stage	π^*_{st1}=2.19
Isentropic efficiency of the 1 stage	η^*_{ad1}=0.871
Total pressure ration of the 2 stage	π^*_{st2}=1.695
Isentropic efficiency of the HPC2	η^*_{ad}=0.875
Total pressure ratio of the HPC2	π^*_C=3.71

HPC2 compressor consists of 5 blade rows: IGV (Z=68, $\bar{h}$=4.2), R1 rotor (blisk) (Z=28, $\bar{h}$=1.04) and S1 stator (Z=68, $\bar{h}$=1.50). IGV and S1 stator vanes are variable ($\Delta\vartheta$IGV=-33°÷+3 and $\Delta\vartheta S_1$=-15°÷+3°). R2 rotor (blisk) (Z=56, $\bar{h}$=1.17) and S2 stator, manufactured as monoblock (Z=68, $\bar{h}$=1.09).

Viscous flow calculations in the compressor (5 blade rows) are based on corrected flow parameters at the inlet (T*=288K, P*=101325 Pa).

The objective of calculations is determination of characteristics of the compressor for six operating modes (at 100%, 95%, 90%, 80%, 70% and 60% rotational speeds).

The following tip clearances are taken into account in the calculations: 0.5 mm – in IGV at the tip and at the hub; 0.5 mm – above the R1 and R2 and 0.5 mm - under the outlet variable stator.

Flow patterns in the stage are shown below.

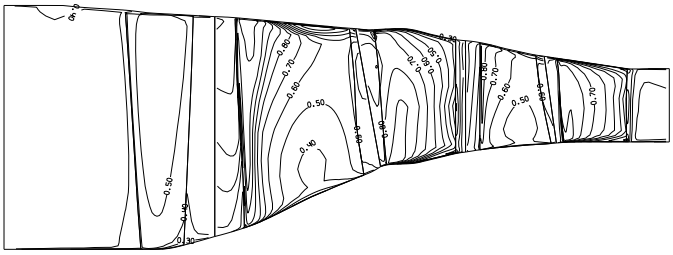

Fig. 1.1.a. Mach number contours on the rotor pressure side and the stator suction side; increment = 0.1

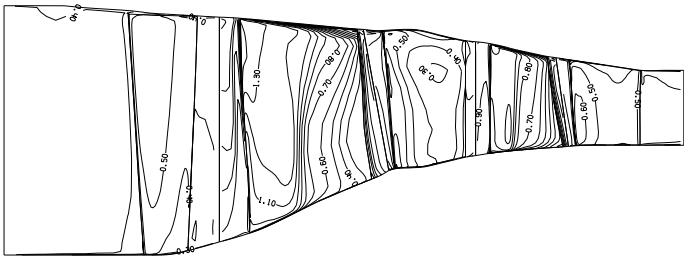

Fig.1.1.b Mach number contours on the rotor suction side and the stator pressure side; increment = 0.1

By optimal variation of IGV and stator vanes, the values of efficiency are supported at a high level and equal to η^*_{ad} =0.88÷0.89 within the range of $\bar{n}_{cor}$=0.6÷0.95. An increase in rotational speeds to $\bar{n}_{cor}$=1.0 results in a decrease in efficiency down to η^*_{ad} =0.875 (designed value) or even to η^*_{ad}=0.83 at $\bar{n}_{cor}$=1.05.

The surge margin from the optimum point to stall at $\bar{n}_{cor}$=0.7 is ΔSM=23%, and then it decreases down to ΔSM=17% at $\bar{n}_{cor}$=0.95, and at $\bar{n}_{cor}$=1.0 it equals to ΔSM=12%.

After finishing the design work bladed rows of experimental compressor HPC2 were manufactured. The HPC2 complicated design allows performing measurements not only local and integral flow parameters but also advanced study of rotors clocking effect (variations R2 blades angular position versus R1) and stators clocking effect (variations S2 blades angular position versus S1). Fig. 1.2 - 1.5 show S1 blades and bladed rows R1, R2 and S2 in assembly.

The comparison of calculated and experimental HPC2 performances, demonstrating good correspondence, is shown below (Fig. 1.6 – 1.7).

Fig. 1.2. Rotor of first stage in assembly

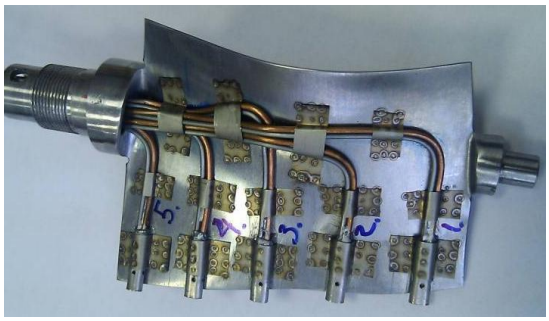

Fig. 1.3. S1 blade, instrumented by deflectors with total pressure tubes and thermocouples

Fig. 1. 4. Rotor of second stage in assembly

Fig. 1.5. S2 stator blades – monoblock, instrumented by strain gauges and total pressure and temperature sensors

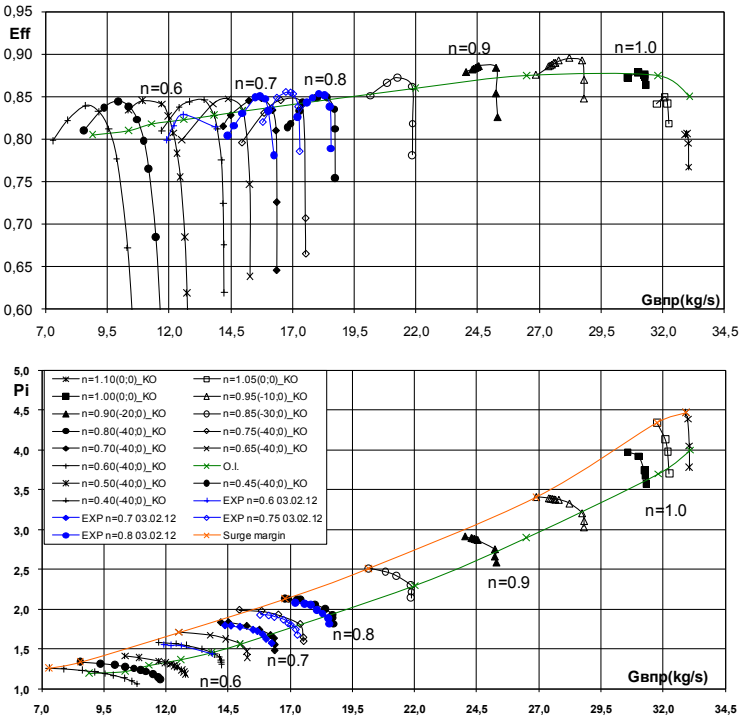

Fig. 1.6 Comparison of calculated and experimental HPC2 performances

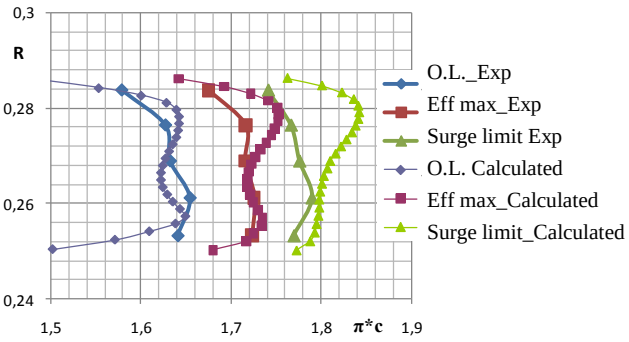

Fig. 1.7 a) Comparison of calculated and experimental local HPC2 performances (Pressure ratio), n=70%

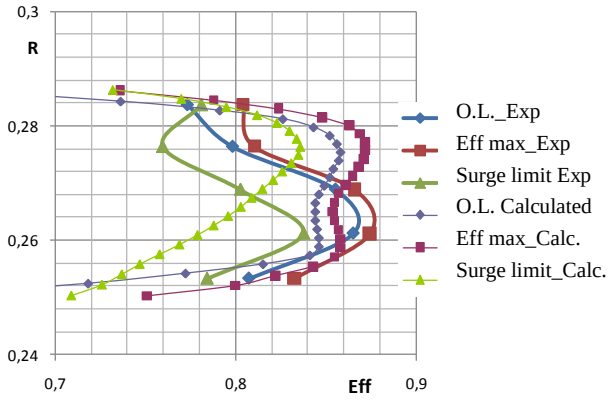

Fig. 1.7 b) Comparison of calculated and experimental local HPC2 performances (Efficiency), n=70%

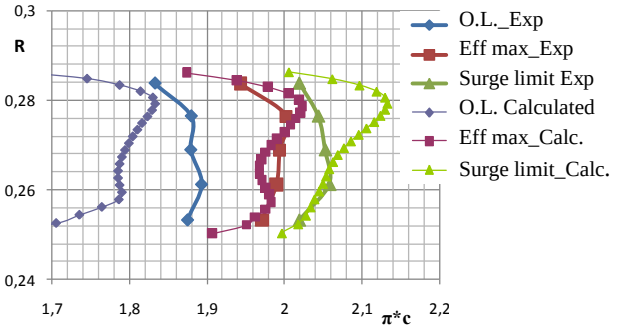

Fig. 1.7 c) Comparison of calculated and experimental local HPC2 performances (Pressure ratio), n=80%

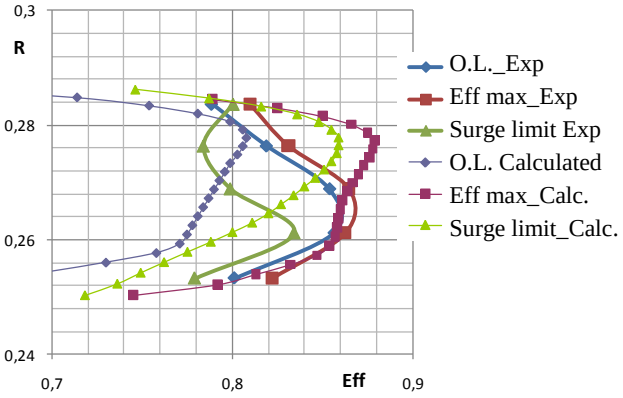

Fig. 1.7 d) Comparison of calculated and experimental local HPC2 performances (Efficiency), n=80%

2. Modification of HPC R1 at $\bar{n}$=100% and 0.4mm tip clearance

For application in multistage compressor system with z=8 the task was stated – to increase the efficiency of each HPC stage on $\Delta\eta^*_{ad}$=1%. For solution of this task the technology of construction 3D bladed row surfaces realizing specified load distribution at blade pressure and suction side on base of 3D inverse problem has been applied. Current paper represents only an example of first stage optimization on base of 3D inverse problem solution for rotor and stator rows in HPC2 designed point at $\bar{n}$=100% at decreased circumferential speed U_{1R} =416 m/s and pressure ratio of HPC2 $\pi^*_c \approx 3.5$. Optimization of other HPC2 rows has been also performed on base of 3D inverse problem solution. Modification of the 1st stage R1 is based on the 3D inverse problem solution by "3D-INVERSE.EXBL" software package. However, prior to R1 redesigning, it is necessary to analyze its operation in the HPC structure (z=8) based on the direct problem solution by the three-dimensional viscous through-flow calculations for a total compressor system. To this effect, the updated "3D-IMP-MULTI" software (3D Navier-Stokes equations, k-ω differential turbulence model, wall functions) developed by CIAM's Compressor Division is used for calculations of local and integral HPC performances.

The objective of these calculations is analysis of flow in the initial HPC version and effects of all modified blade rows on HPC performances at 100% rotational speed (n_{cor}=100%, u_{1R} = 416 m/s). Calculations of viscous flow in the compressor (17 blade rows, including inlet guide vanes) are completed at corrected parameters at the inlet (T* = 288°K, P* = 101325 Pa).

Designing of HPC blade rows and calculations of integral performances take into account that nominal (100 %) tip clearances are 0.4 mm at R1÷R8 tips, at variable IGV and S1 tips and hubs and at the hub of cantilevered S2÷S7 blades. S8 vanes are shrouded.

The operating point at $\bar{n}_{cor}$=100% and 0.4-mm tip clearance is chosen on the characteristic line of the initial HPC version for R1 redesigning. The three-dimensional viscous through-flow calculations of the flow in the HPC in the «mixing plane» approximation show that HPC R1 operation at this point corresponds to the left branch of the characteristic. It means that there is a detached shock at the R1 inlet in the tip and max. loading is near to R1 leading edge. Rotor 1 in the HPC system provides the following parameters: π^*_{R1} = 2.184, $\eta^*_{ad.R1}$ = 0.895.

Fig. 2.1.a shows that intensive flow acceleration with subsequent deceleration in the detached shock takes place on the R1 suction side. The

supersonic zone in the R1 tip section is closed by shock with Mach-number= 1.42 before the shock (see Fig. 2.1.c). As evident from Fig. 2.2a, there is a wide separation zone in the HPC R1 hub sections that covers approx. 30 % of the blade height in the vicinity of the leading edge. This separation zone is caused by high incidence angles on the R1 leading edge. Improvement of R1 aerodynamics, namely, its redesign aiming at shifting the detached shock into the blade channel with simultaneous elimination of the separation zone in the vicinity of R1 leading edge at the hub is the basic provision for improvement of compressor performances and, first of all, the surge margin. As can be seen in Fig. 2.1.a, the operating point of the initial HPC version at the nominal clearance value is located on the left branch of the HPC characteristic. In this region there is a risk of unstable HPC operation that can result in strong fluctuations of the detached shock and HPC surge.

At first, «3D-IMP-MULTI» software package is used for calculation of 3D viscous flow in the operating point in the total HPC system, including R1 [3-5]. Based on this calculation, loading of the initial R1 blade is found. Loading of R1 blade means a static pressure difference between pressure and suction sides in the face centers of cells with respective numbers and located on corresponding blade surfaces.

The analysis of Fig. 2.1.c and Fig. 2.1.e shows that max. loading at the tip for the initial R1 version is observed near to the leading edge where the detached shock wave is located. Max. loading for the modified R1 version (Fig. 2.1.d and Fig. 2.1.f) is found in the blade channel, nearer to the R1 trailing edge. Distribution of initial and modified loadings along R1 blade height is shown in Fig. 2.3-2.4.

Modification of loading in the initial version shown in Fig. 2.3-2.4 is based on condition that loads in corresponding sections of initial and modified versions should be equal. It means equality of areas between the curves corresponding to distributions of static pressure on blade suction and pressure sides for initial and modified versions.

The analysis of Fig. 2.3 shows that extremely high spike of max. loading in the vicinity of R1 leading edge at the hub leads to formation of a separation zone on this part of R1 blade. As shown in Fig.2.3, the load peak is cut off to eliminate the separation zone at the R1 hub for modified version.

Modification of R1 is based on solution of a three-dimensional inverse problem [1-3]. Fig. 2.3 - Fig. 2.4 show a scheme of load distribution along the blade chord in various sections for solution of the three-dimensional inverse problem. Fig. 2.1.a and Fig. 2.1.b show flow in R1 near to the operating point in conditions with the detached shock for the HPC version with the initial R1 and with the modified R1 after solution of the three-dimensional inverse problem. Parameters of this point were listed above.

CIAM's «3D-INVERSE.EXBL» software package is used for solution of the 3D inverse problem. The value of modified load is used as boundary conditions for construction of surfaces of the modified blade on the basis of the 3D inverse problem solution. Flow parameters in the centers of the bordering cells found by the solution of the direct problem are used as boundary conditions at the inlet and the outlet of the computational domain for any blade row.

Fig. 2.1. - Fig. 2.2 show the comparison of initial and modified R1 versions by the example of Mach number distribution in several R1 sections from the hub to the tip. Additionally, distributions of isentropic Mach number (the tip section) and static pressure relatively to critical dynamic pressure of incoming flow are shown in these R1 sections.

As evident from Fig. 2.2.b, an extensive separation zone at the hub of the initial blade is eliminated after solution of the 3D-inverse problem.

Fig. 2.1.a and Fig. 2.1.b also demonstrate the presence of a detached shock for the initial version and the shock closure inside the blade channel for the modified version after the solution of the 3D-inverse problem.

The initial R1 version at $\bar{n}_{cor}$=100% operating point provides the following parameters: π^*_{R1}= 2.184, $\eta^*_{ad.R1}$=0.895.

The further R1 optimization is aimed at an increase in R1 efficiency above $\eta^*_{ad.R1} \geq 0.91$ and its $\pi^*_{R1} > 2.22$. For this purpose

optimization with various number of R1 blades is completed, in particular, R1 versions with 25 and 21 blades are studied. Subsequent 3D-calculations of the total HPC system show that in respect of an increase in efficiency, pressure ratio and, first of all, corrected air flow, the optimum R1 version has 21 blades. It is obvious that this R1 version is higher loaded (Nag_t = 0.055553) as compared with R1 version with 25 blades (Nag_t = 0.043859). It is reasonable that additional corrections in static pressure distribution along the blade profile are required for the purpose of more uniform load distribution along R1 blade chord to improve, mainly, R1 efficiency. An example of this static pressure correction is shown in Fig. 2.5 and Fig. 2.6. As a result of optimization on the basis of 3D-inverse problem solution, there are immediate gains both in R1 pressure ratio and its efficiency: $\pi^*_{R1} = 2.251$, $\eta^*_{ad.R1} = 0.917$.

Then, the initial R1 blade is replaced in HPC by the modified R1 blade found by solution of the 3D inverse problem. After that, the modified HPC performances (analyzed in Section 4) are found on the basis of 3D direct problem solution.

Initial HPC R1 blade version | Modified HPC R1 blade version

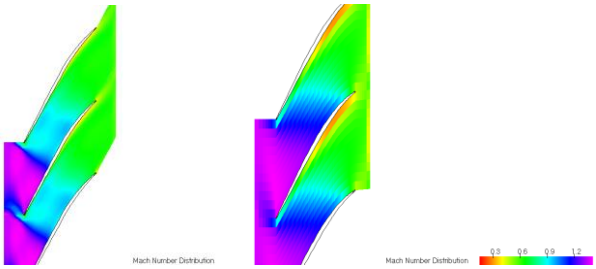

a) b)

Isentropic Mach number distribution along the blade profile

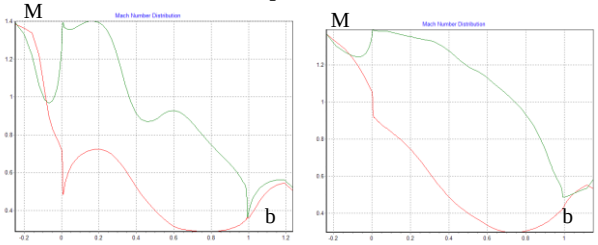

c) d)

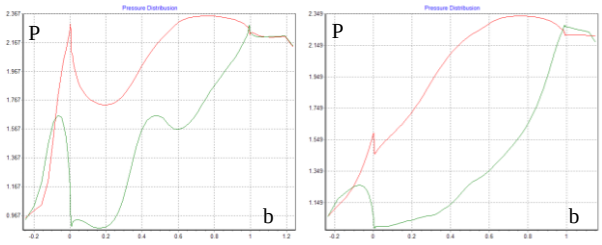

e) f)

Static pressure distribution along the blade profile

Fig. 2.1 Comparison of Mach number and static pressure distributions for initial and modified HPC R1 versions

Blade section: 98% of blade height; $\bar{n}$=100%

Initial HPC R1 blade | Modified HPC R1 blade

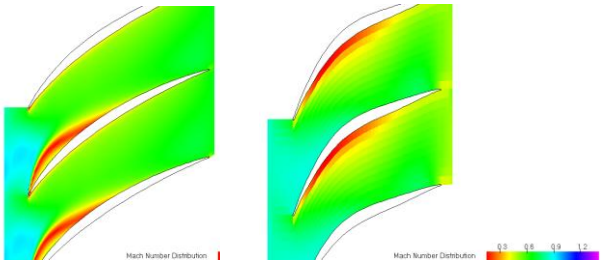

a) b)

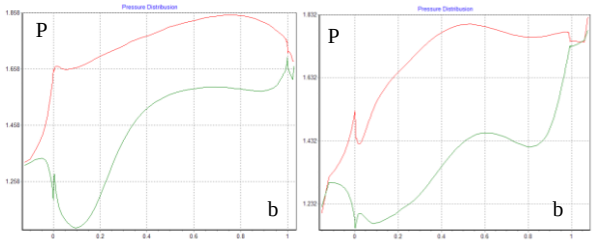

c) d)

Static pressure distribution along the profile

Fig. 2.2 Comparison of static pressure distributions for initial and modified HPC R1 versions

Blade section: 3% of blade height; $\bar{n}$ = 100%

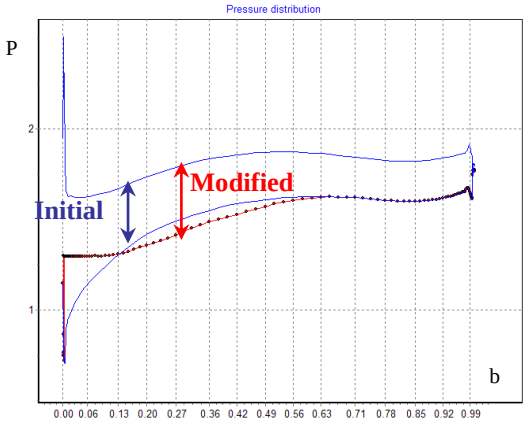

Fig. 2.3 HPC R1. Section: 3% of blade height; $\bar{n}$ = 100%

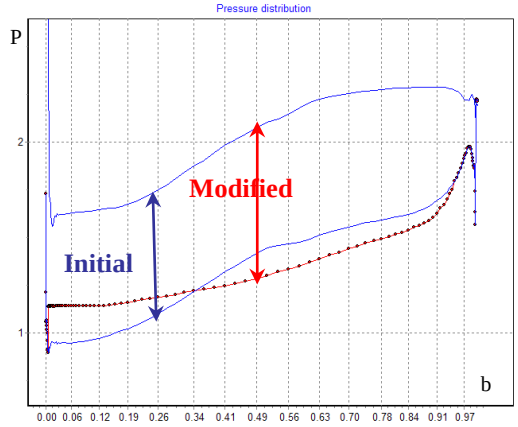

Fig. 2.4 HPC R1. Section: 98% of the blade height; $\bar{n}$ = 100%

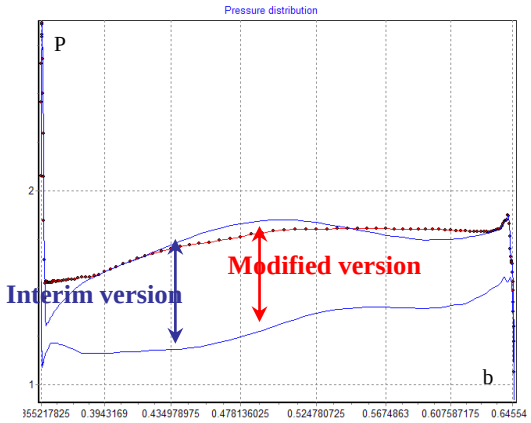

Fig. 2.5 HPC R1. Blade section: 3% of blade height; $\bar{n}$ = 100%

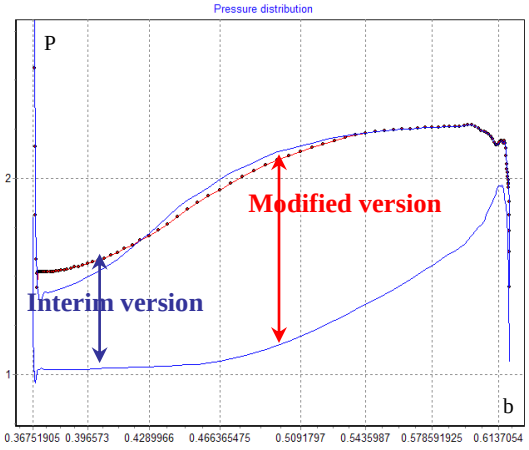

Fig. 2.6 R1 HPC. Blade section: 79% of blade height; $\bar{n}$ = 100%

3. HPC S1 Modification at $\bar{n}$=100% operating point

Modification of the 1st stage stator (S1) is based on the 3D inverse problem solution by "3D-INVERSE.EXBL" software package. Prior to S1 redesigning it is necessary to analyze its operation in the HPC structure based on the direct problem solution by three-dimensional viscous through-flow calculations of the flow in the total compressor system.

An operating point on the initial HPC characteristic line is chosen at $\bar{n}_{cor}$=100% for S1 redesigning. S1 in this point of the initial HPC version is operating on the left branch of the characteristic line. It means that incident flow angles at the S1 inlet are high with formation of a local supersonic zone in the vicinity of the S1 leading edge and max. load is very near to S1 leading edge. S1 in the HPC system provides σ_{S1} = 0.98.

Improvement of S1 aerodynamics, namely, its redesign aiming at a decrease in S1 load by its more uniform distribution along the vane height is the basic provision for an improvement of compressor performances and, first of all, its surge margin.

At first, «3D-IMP-MULTI» software package is used for computation of 3D viscous flow at the operating point for the total HPC system, including S1. Based in this computation, loading of the initial S1 vane is found. Loading of the S1 vane means a difference between static pressures on the suction and pressure sides in the face centers of cells with corresponding numbers and located on a respective vane surface.

Loading in the initial version shown in Fig. 3.1 and Fig.3.2 is corrected under the condition of loading equality in corresponding sections of initial and modified versions. It means equality of areas between lines corresponding to static pressure distributions on pressure and suctions sides for the initial and modified versions.

The analysis of Fig. 3.1 and Fig. 3.2 shows that max. load for the initial S1 version is found near to the leading edge in the region of high incident angles of incoming flow. Max. loading near to the leading edge for the modified S1 version is considerably reduced by its redistribution towards the center the S1 vane channel. Distribution of the initial and modified loading along S1 vane height is shown in Fig. 3.1 and Fig. 3.2. Loading distribution along the vane height in sections between the S1 vane tip and hub is very close to linear.

Fig. 3.3 and Fig. 3.4 show the comparison between the initial and modified S1 versions by

the example of Mach number distributions in various S1 sections - from the hub to the tip. Additionally, distributions of isentropic Mach number and static pressure relatively to the critical dynamic pressure of incoming flow are shown in these S1 sections.

As well illustrated by Fig. 3.3 and Fig. 3.4, there are high gradients of flow parameters in the vicinity of the leading edge and more smoothed gradients of flow parameters in the vane channel in the modified S1 version after 3D-inverse problem solution.

The subsequent S1 optimization is aimed at elimination of a supersonic zone near to the S1 leading edge as well as a more uniform distribution of aerodynamic loading along the S1 vane chord for the purpose of an increase in surge margin of the total HPC system.

Certainly, it calls for additional corrections in static pressure distribution along the vane profile for the purpose of more uniform distribution of loading along the vane to keep a high level of σ_{S1}. Fig. 3.3 and Fig. 3.4 show the result of S1 optimization on the basis of static pressure corrections presented in Fig. 3.1 and Fig 3.2.

Regardless the fact that loading distribution along the S1 vane chord is more uniform, total pressure recovery ratio (σ_{S1}) is almost unchanged: σ_{S1} = 0.978. More uniform load distribution along the S1 vane chord has a noticeable effect on an increase in surge margins of the 1st stage and the HPC as a whole.

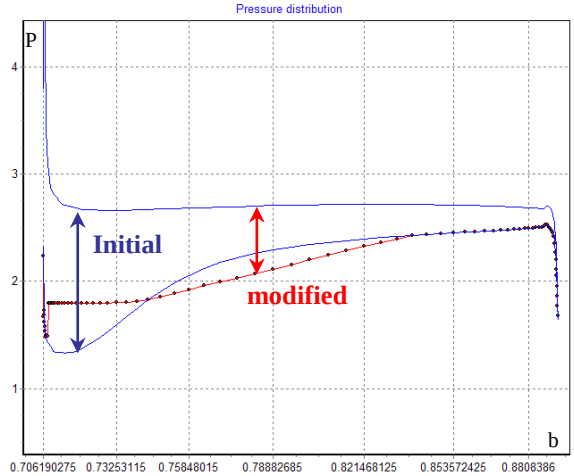

Fig. 3.1 HPC S1. Section: 3% of the vane height; $\bar{n}$ = 100%

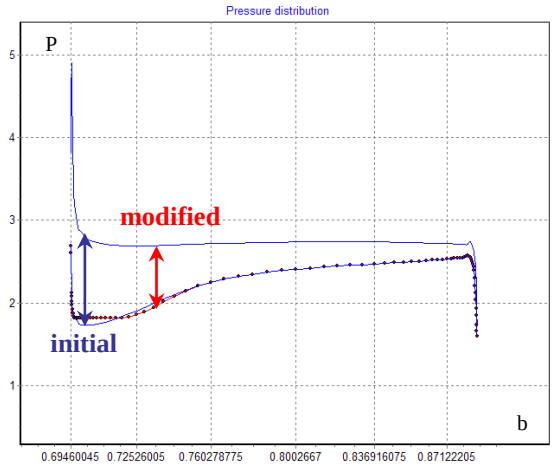

Fig. 3.2 HPC S1. Section: 98% of the vane height; $\bar{n}$ = 100%

Initial HPC S1 vane Modified HPC S1 vane

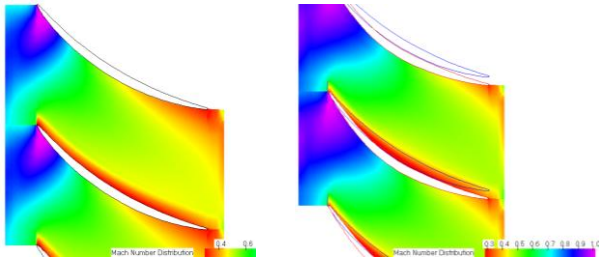

a) b)

Isentropic Mach number distribution along the profile

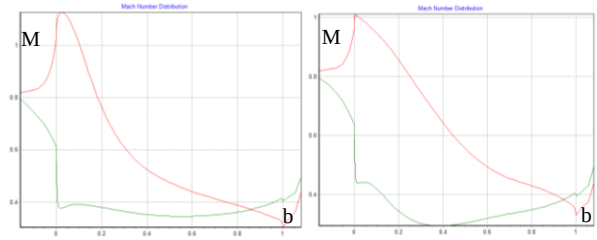

c) d)

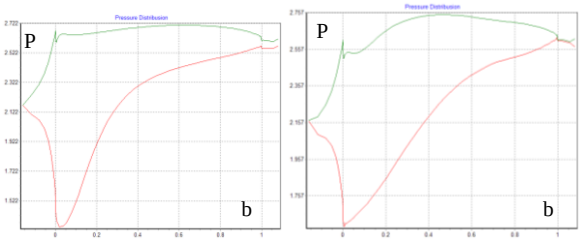

e) f)

Static pressure distribution along the profile

Fig. 3.3 Comparison of Mach number and static pressure distributions for initial and modified HPC S1

Section: 3% of the vane height; $\bar{n}$ = 100%

Initial HPC S1 vane Modified HPC S1 vane

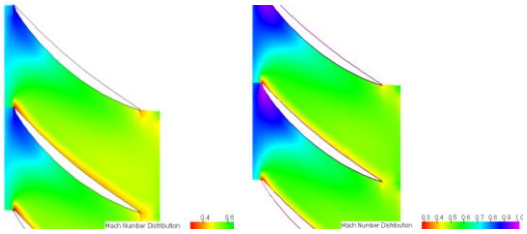

a) b)

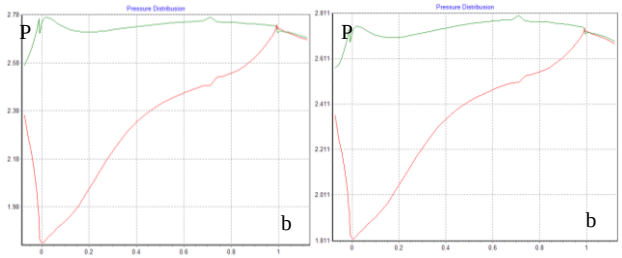

c) d)

Static pressure distribution along the profile

Fig. 3.4 Comparison of static pressure distributions for initial and modified HPC S1 versions
Blade section: 98% of blade height; $\bar{n}$=100%

4. Operability of the modified first stage as a component of HPC and comparison of calculated and experimental data

Upon completion of optimization on the basis of 3D inverse problem solution the first stage is installed in the eight-stage HPC. 3D viscous flow in all HPC blade rows is re-calculated by "3D-IMP-MULTI" package. Calculated data at 0.4-mm tip clearance are presented in Fig. 4.1 and Fig.4.2. The results show that the goal of redesigning is achieved and the modified stage at $\bar{n}$ = 100% is operable with the shock inside the blade channel that makes implementation of design flow conditions possible within the total HPC system.

Fig. 4.1 and Fig.4.2 show first three MP1, MP2 and MP3 surfaces in which boundary conditions in «mixing plane» approximation are used. It is worth noting that the 3D inverse problem is solved for an individual HPC blade row that needs in improvement of flow and, respectively, its integral parameters. To ensure matching of blade rows in the HPC system, the boundary conditions for solution of 3D inverse problem are taken from the direct problem solution by 3D viscous through-flow calculations of the flow in HPC.

For example, in the solution of 3D inverse problem for the purpose of R1 optimization the left computational domain border coincides with MP1 surface, and the right border - with MP2 surface (see Fig. 4.1 and Fig.4.2). In the solution of 3D inverse problem for the purpose of S1 optimization the left computational domain border coincides with MP2 surface, and the right border - with MP3 surface (see Fig. 4.1 and 4.2). When solving the inverse problem, boundary conditions for flow on MP1, MP2 and MP3 surfaces coincide with corresponding boundary conditions in the «mixing plane» approximation in the direct problem solution.

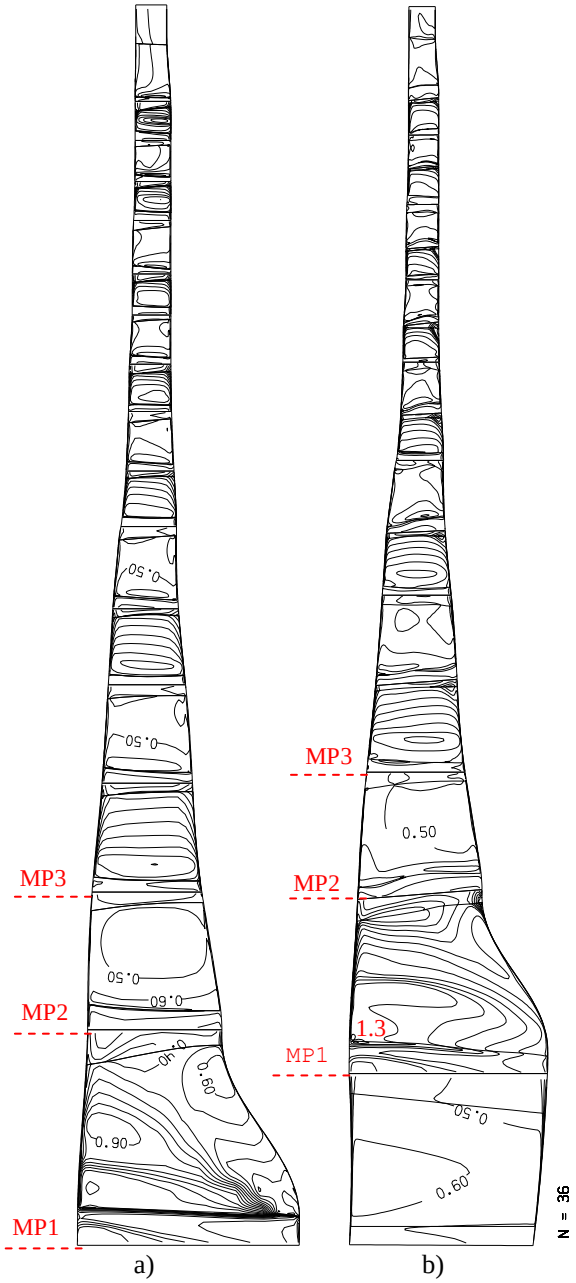

a) b)

Fig. 4.1 Mach number distribution along rotor suction side and stator pressure side a) – initial version, b) – modified version

As shown in Fig. 4.1.a and 4.1.b, results of 3D viscous through-flow calculations of the flow in the eight-stage HPC with the optimized first stage on the basis of 3D inverse problem solution give the evidence for achievement of HPC design parameters: elimination of a detached shock at the first stage inlet (along the

R1 blade height, h> 40%) as well as a separation zone at the R1 hub.

The comparison of calculated and experimental data of pressure ratio distributions and increments in total temperature measured by sensors mounted to HPC S1, S2 and S3 leading edges show their good agreement.

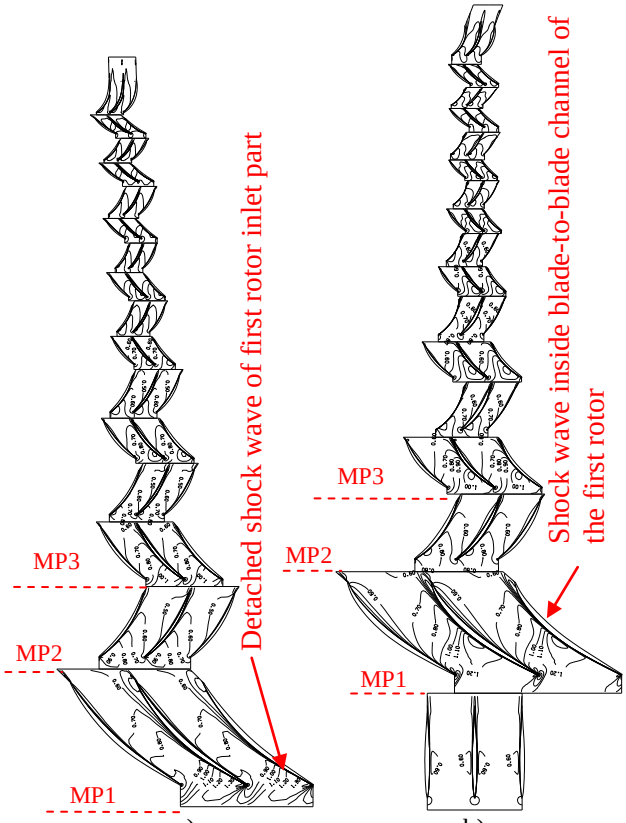

a) b)

Fig. 4.2 Mach number distribution on middle section of HPC ($\bar{h}$=50%) a) – initial, b) – modified

Total pressure and temperature are measured by 5 Pitot tubes and temperature sensors equally spaced along height of stator vanes.

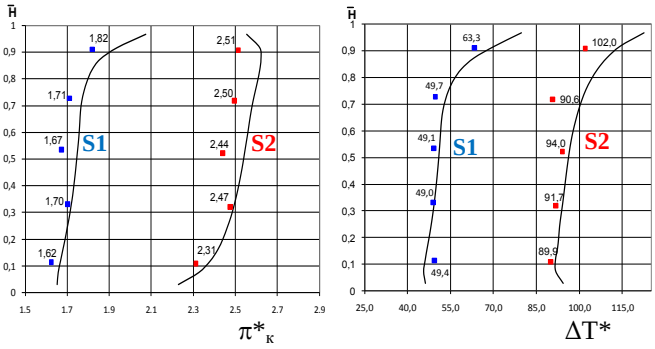

a) b)

Fig. 4.3 HPC n=90%

a) – pressure ratio π^*_c, b) – $\Delta T^*=T^*-T^*_{inlet}$

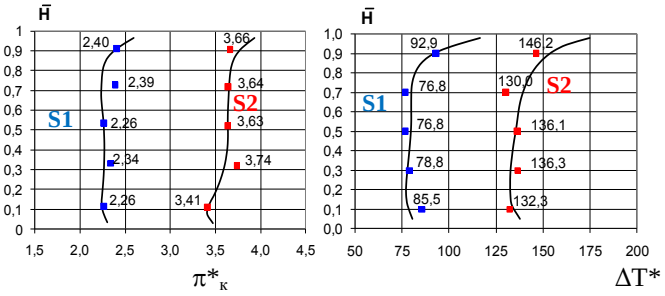

a) b)

Fig. 4.4 HPC n=100% a) – pressure ratio π^*_C, b) – $\Delta T^*=T^*-T^*_{inlet}$

■ ■ – experiment, ——— - calculations

The comparison of calculated and experimental data of total pressure and temperature, measured by 5 Pitot tubes and temperature sensors, are represented in Fig. 4.3 and Fig.4.4.

Conclusions

1. Numerical and experimental investigations are presented for a high-loaded two stages compressor HPC2 that provides the following parameters at $\bar{n}_{cor}$=100%, U_{R1tip}=441 m/s: π^*_c=3.7 pressure ratio at $\bar{d}_1$=0.65 relative hub diameter. This stage was tested at CIAM's C-3 test facility. The comparison of calculated and experimental data shows their good agreement.

2. Two stages compressor HPC2 was inserted into an eight-stage HPC and used as its first and second stages. Through-flow calculations of 3D viscous flow in all rows of the eight-stage HPC show that R1 operation lies on the left branch of the HPC characteristic line. It means that there is a detached shock at R1 inlet and max. loading is very near to the R1 leading edge. Moreover, the analysis of 3D viscous calculations shows that there is a wide separation zone in hub sections of HPC R1 that covers approx. 30% of blade height in the vicinity of the leading edge. R1 in HPC system provides the following parameters: π^*_{R1}=2.184, η^*_{ad}=0.895. The separation zone is caused by high incidence angles at the R1 leading edge.

3. To improve R1 aerodynamics, the rotor was redesigned for the purpose of shifting the detached shock into the blade channel with simultaneous elimination of the separation zone in the vicinity of R1 leading edge in hub sections. Modifications of R1 and S1 were

based on the solution of a three-dimensional inverse problem by means of «3D-INVERSE.EXBL» software package.

4. Results of the through-flow calculation of 3D viscous flow in the eight-stage HPC with the optimized first stage on the basis of 3D inverse problem solution give the evidence of achievement the HPC design parameters: elimination of the detached shock at the first stage inlet (along the R1 blade height, h>40%) as well as the separation zone at the R1 hub and increase of modified HPC2 efficiency in HPC systemon more than $\Delta\eta^*_{ad} \geq 1\%$. The comparison of calculated and experimental data of pressure ratio distributions and increments of total temperature measured by sensors mounted on HPC S1, S2 and S3 leading edges show their good agreement.

References

[1] V.I. Mileshin, I.K. Orekhov, S.V. Pankov. "Numerical and experimental Investigations of bypass fans characteristics". *Proceedings of ISABE International Conference*, Bejing, Chine, ISABE-2007-1138, 2007.

[2] V.I. Mileshin, I.K. Orekhov, S. K. Shchipin, A.N. Startsev. "New 3D inverse Navier-Stokes based method used to design turbomachinery blade rows". *Proceedings of HT-FED Conference*, Charlotte, North Carolina, USA, HT-FED-2004-56436, 2004.

[3] V.I. Mileshin, I.K. Orekhov, S. K. Shchipin, V.A. Fateyev. "Effect of tip clearance on flow structure and integral performances of six-stage HPC". *Proceedings of ISABE International Conference*, Bejing, Chine, ISABE-2007-1179, 2007.

[4] V.I. Mileshin, I.K. Orekhov, S.K. Shchipin and A.N. Startsev. "3D inverse design of transonic fan rotors efficient for a wide range of RPM". *Proceedings of ASME Turbo Expo Conference*, Montreal, Canada, GT2007-27817, 2007.

[5] V.I. Mileshin, M.A. Nyukhtikov, S.V. Pankov, S.K. Shchipin, I.K. Orekhov. "Open counter – rotating fan blades optimization based on 3D inverse problem Navier-Stokes solution method with the aim of tonal noise reduction". *Proceedings of ASME Turbo Expo Conference*, Berlin, Germany, GT2008-51173, 2008.

Copyright Statement